

A $z = 3.045$ Ly α emitting halo hosting a QSO and a possible candidate for AGN-triggered star formation^{*}

Michael Rauch,^{1†} George D. Becker,² Martin G. Haehnelt,² Robert F. Carswell²
and Jean-Rene Gauthier³

¹*Carnegie Observatories, 813 Santa Barbara Street, Pasadena, CA 91101, USA*

²*Institute of Astronomy and Kavli Institute for Cosmology, Cambridge University, Madingley Road, Cambridge CB3 0HA, UK*

³*California Institute of Technology, Pasadena, CA 91125, USA*

Accepted 2013 January 24. Received 2013 January 18; in original form 2012 December 17

ABSTRACT

In this third paper in a series on the nature of extended, asymmetric Ly α emitters at $z \sim 3$ we report the discovery, in an ultra-deep, blind, spectroscopic long-slit survey, of a Ly α emitting halo around a QSO at redshift 3.045. The QSO is a previously known, obscured active galactic nucleus (AGN). The Ly α emitting halo appears extended along the direction of the slit and exhibits two faint patches separated by 17 proper kpc in projection from the QSO. Comparison of the two-dimensional spectrum with archival *Hubble Space Telescope* ACS images shows that these patches coincide spatially with emission from a peculiar, dumbbell-shaped, faint galaxy. The assumptions that the Ly α emission patches are originating in the galaxy and that the galaxy is physically related to the QSO are at variance with photometric estimates of the galaxy redshift. We show, however, that a population of very young stars at the redshift of the QSO may fit the existing rest-frame broad-band UV photometry of the galaxy. If this scenario is correct, then the symmetry of the galaxy in continuum and Ly α emission, the extension of the QSO's Ly α emission in its direction, and the likely presence of a young stellar population in close proximity to a (short-lived) AGN suggest that this may be an example of AGN feedback triggering external star formation in high-redshift galaxies.

Key words: galaxies: evolution – galaxies: haloes – galaxies: interactions – intergalactic medium – quasars: general – diffuse radiation.

1 INTRODUCTION

Lyman α emitting haloes around QSOs are a well-documented and theoretically expected (e.g. Haiman & Rees 2001) consequence of the enhanced ionization of the surrounding gas by the central active galactic nuclei (AGN). In contrast, the impact of AGN on star formation in the QSO host galaxy or its satellite galaxies is more complex and subject to ongoing debate. Most recently, the study of AGN feedback has focused on the quenching of star formation (e.g. Silk & Rees 1998; Fabian 1999; Schawinski et al. 2009; Farrah et al. 2012; Maiolino et al. 2012). However, considerable observational evidence (e.g. van Breugel et al. 1985; Chambers, Miley & van Breugel 1987; McCarthy et al. 1987; Dey et al. 1997; Croft et al. 2006) and theoretical arguments (e.g. De Young 1981, 1989; Begelman & Cioffi 1989; Rees 1989; Mellema, Kurk & Röttgering 2002;

Fragile et al. 2004; Silk 2005) suggest that AGN can also induce the formation of stars in their host galaxies. The influence of the AGN may extend beyond mere enhancement of the star formation rate and create peculiar stellar morphologies (e.g. Gaibler et al. 2012), perhaps even in satellites of the host galaxy (e.g. Efremov 2012).

In this paper we report the discovery, in a deep spectroscopic search for extended Ly α emission, of an extended asymmetric Ly α halo around the $z = 3.045$ obscured QSO J033238.76–275121.6. Inspection of existing *Hubble Space Telescope* (HST)/ACS images shows spatial structure in the halo's Ly α profile coinciding in projection along the slit with a peculiarly shaped, double-lobed galaxy. Although the redshift of the galaxy is uncertain, we present arguments that suggest that the galaxy may be at the redshift of the QSO. We show that this would require a very young stellar population, the age of which would be unlikely to be synchronized with the short-lived AGN activity if there were no causal connection between the two, possibly in the form of QSO feedback triggering the formation of the stars in the external galaxy. This scenario may also provide a plausible resolution to the problem posed by the divergent photometric redshifts suggested in the literature for the galaxy.

^{*} This paper is based on data gathered with the 6.5 m Magellan Telescopes located at Las Campanas Observatory, Chile.

[†] E-mail: mr@obs.carnegiescience.edu

Table 1. Properties of the QSO (A) and the object (B&C).

ID	z_{spec}	z_{phot}	GOODS ⁱ	V^i	$B - V^i$
A	3.045 ^a , 3.951 ^b	2.51 ^c , 1.46 ^d , 2.970 ^e , 1.663 ^f , 3.001 ^g	J033238.76–275121.6	26.32 \pm 0.05	1.41 \pm 0.23
B&C	3.045 ^a	1.560 ^h , 2.310 ⁱ	J033238.88–275119.5	26.55 \pm 0.09	0.31 \pm 0.173

Comments: ^athis paper; ^bVanzella et al. (2010); ^cZheng et al. (2004); ^dTreister et al. (2006); ^eBrusa et al. (2009); ^fCardamone et al. (2010); ^gLuo et al. (2010); ^hGrazian et al. (2006); ⁱGiavalisco et al. (2004).

2 OBSERVATIONS

2.1 Spectroscopy and archival imaging

The object in question is the third of several extended Ly α emitters in the long-slit blind spectroscopic survey described in our earlier papers (Rauch et al. 2011, Paper I; Rauch et al. 2013, Paper II). A 2 arcsec wide long slit was placed for a total observing time of 61.4 h at a random position centred on the *Hubble Ultra-Deep Field*, with a position angle of 0°. The slit happened to intersect at least partly the object known as GOODS J033238.76–275121.6 (Giavalisco et al. 2004) or Combo-17 26280 (Wolf et al. 2001), which has an absorption-corrected, rest-frame X-ray (0.5–8 keV) luminosity of 9.22×10^{43} erg s^{−1} (Xue et al. 2011). Taken together with its hardness ratio and red optical colours this suggests classification as a type 2 AGN or obscured, borderline QSO (e.g. Padovani et al. 2004; Szokoly et al. 2004). A range of redshift estimates exist in the literature (see Table 1), including a spectroscopic redshift of

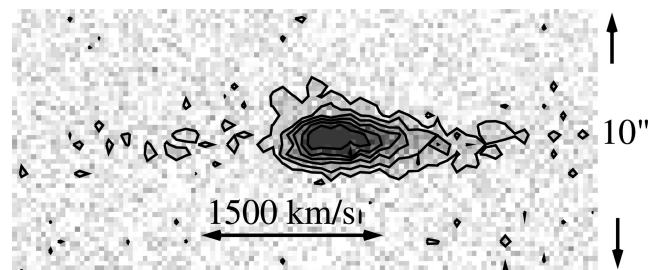


Figure 1. LDSS3 spectrum of the QSO's Ly α emission line region. Flux density contours are plotted on top of the flux density spectrum, to give an idea of the noise and the dynamic range of the data. Wavelength (or redshift) increases from left to right. The direction along the slit is precisely N-S, with N on top. The outermost contiguous contour corresponds to a flux density of 7×10^{-20} erg cm^{−2} s^{−1} Å^{−1}. The largest distance of this contour from the (very faint) QSO continuum along the slit is about 2.2 arcsec, or 17 proper kpc.

$z = 3.951$ (Vanzella et al. 2010). In our spectrum the QSO has a spatially asymmetric Ly α emission line peaking near 4920 Å, or at a redshift of 3.049. The presence and wavelength position of faint C iv emission suggest a redshift of 3.045, which is lower by about 300 km s^{−1}. Lacking a good estimator of the systemic redshift we adopt the C iv redshift $z = 3.045$ (as the relation between the Ly α position and the systemic redshift is probably even more complicated). The precise redshift is immaterial for the main arguments in this paper. At this redshift, the relative faintness in the observed B band ($B - V = 1.41$), aside from a smaller correction by a factor of 0.8 for absorption by the Lyman α forest, would be mainly due to reddening, consistent with a moderate amount of intrinsic extinction ($A_V \sim 0.7$) in the QSO's rest-frame V band. With our new, lower redshift, the flux measured for this object by Vanzella et al. (2010) in a filter designed to capture escaping Lyman continuum radiation at $z \sim 4$ would be explained by an overlap of the filter band with the QSO's (less strongly absorbed) non-ionizing continuum.

Even though the existing photometry shows the QSO to have a V -band magnitude of 26.31 (Giavalisco et al. 2004), the continuum of the object is barely visible in our spectrum, suggesting that much of the light from the QSO may not have gone through the 2 arcsec wide slit.

The spectral profile of the Ly α emission line peak is asymmetric, with a red shoulder, a steep drop going bluewards, and some faint emission at the bluest end (Fig. 1). The total flux transmitted through the slit is $(5.4 \pm 1.1) \times 10^{-17}$ erg cm^{−2} s^{−1}. The emission line is spatially asymmetric as well, with the flux extending further out to the N (top in Fig. 1). The lowest discernible flux density contour in the 2D spectrum (Fig. 1), at 7×10^{-20} erg cm^{−2} s^{−1} Å^{−1}, extends out to about 17 proper kpc, encompassing two faint point-like emission peaks shown as '1' and '2' in Fig. 2, with individual Ly α fluxes $(7.1 \pm 2.1) \times 10^{-19}$ and $(7.8 \pm 1.5) \times 10^{-19}$ erg cm^{−2} s^{−1}, i.e. 3.5σ and 5.2σ detections, respectively. These faint features can still be discerned separately in the two subsets of data obtained in 2008 and 2009, suggesting that they are not noise artefacts. Removing the smooth, diffuse halo with a template

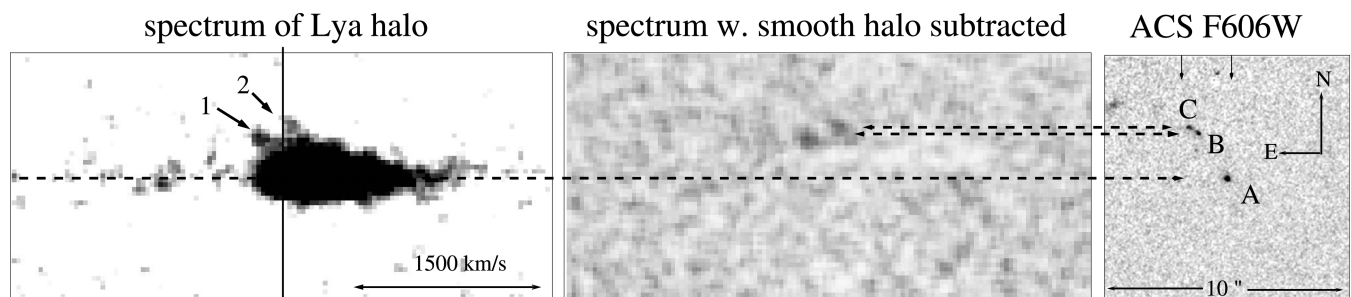


Figure 2. LDSS3 spectrum of the Ly α emission line region (left); same spectrum, but with the smooth QSO halo subtracted (centre), and ACS F606W image (right). The spatial size of the image and the extent of the spectrum along the slit shown here are 10 arcsec. A velocity scale of 1500 km s^{−1} is indicated in the spectrum. The dashed lines are meant to guide the eye and connect the position of the QSO (bottom line, 'A') and the continuum in the spectrum, and the two galaxy components 'B' and 'C' with the two knots 1 and 2 of Ly α emission, respectively. The vertical line in the spectrum approximately indicates the redshift 3.045 derived from the C iv emission line. The two downward arrows at the top of the right-hand panel indicate the approximate E-W positions of the slit jaws.

determined from the spatial profile redwards of the two features reveals them as the only significant remaining features in the spectral range shown (central panel in Fig. 2). The separation in wavelength space between 1 and 2 amounts to about 290 km s^{-1} , and they straddle the adopted ‘systemic’ redshift for the QSO (vertical line in the left-hand panel of Fig. 2). A comparison with the publicly available GOODS-S ACS F606W cutout images (Giavalisco et al. 2004; Fig. 2, right panel) shows, in addition to the image of the QSO (‘A’), two faint continuum emitters (‘B’ and ‘C’) at approximately the same N-S angular distance θ from A [$\theta(B - A) = (1.83 \pm 0.03)$; $\theta(C - A) = (2.11 \pm 0.03) \text{ arcsec}$] that separates the objects 1 and 2 from the continuum trace of the QSO [(1.59 ± 0.20) and $(2.16 \pm 0.20) \text{ arcsec}$, respectively, left-hand panel]. Objects B and C form an apparently dumbbell-shaped structure in the ACS images. With similar broad-band magnitudes in several optical filters, they may in fact be one, spatially coherent object. We shall refer to them as a single structure in what follows but cannot rule out from the existing observations that they are two separate galaxies.

2.2 The object B&C – unrelated foreground galaxy or young starburst at the same redshift as the QSO?

The close alignment of the B&C continuum emission in projection with the faint Ly α emission 1 and 2 in the 2D spectrum may suggest a common origin in the same object. However, the two photometric redshifts for B&C do not agree with the spectroscopic redshift of the Ly α patches (and of the QSO; see Table 1), nor do they agree among themselves. Possible explanations for the discrepancy include the faintness of the object, the difficulty of spatially resolving the contributions from QSO and galaxy in ground-based observations, variable amounts of Ly α emission in the broad-bands, and possibly the absence of templates from the photometric redshift determinations representing what may be an unusual stellar population. In particular, the relatively blue colours of the object would be naturally explained by the properties of a very young/peculiar stellar population at redshift 3.045, as described below. The photometry publicly available for constraining the rest-frame UV colours of the B&C object(s) includes *HST* ACS bands from original GOODS photometry by Giavalisco et al. (2004), ground-based VLT-VIMOS photometry of Grazian et al. (2006) and two additional ground-based *U*-band observations from the European Southern Observatory WFI (the so-called U35 and U38 bands), which were combined into single publicly available images by the GaBoDS group (Hildebrandt et al. 2006). Cardamone et al. (2010) have measured *U*-band fluxes for those images and included them in their catalogue. Although the ground-based WFI images are noisy, these bands are situated close in wavelength to the Lyman limit of the Ly α halo and can at least in principle constrain the redshift of the B&C system. For our analysis below, we adopt these values in addition to the VIMOS *U* band and the ACS images.

For the galaxy to be at the redshift of the QSO, the steepness of the spectrum, even in the non-ionizing continuum, would require the spectrum to be dominated by young stars. The QSO could boost the continuum emitted by the galaxy below the Lyman limit when part of the QSO’s ionizing radiation is ‘reflected’ by neutral hydrogen surrounding the galaxy, but the flux of the QSO seems to fall short by considerable amounts for this to work. Moreover, unless the gas is optically thin, the effect would also produce a reflected, proportional two-photon continuum redwards of Ly α that would tend to flatten the continuum slope. We thus attempted to fit the broad-band optical measurements of objects B&C with a young starburst spectrum at the redshift of the QSO, using the library of

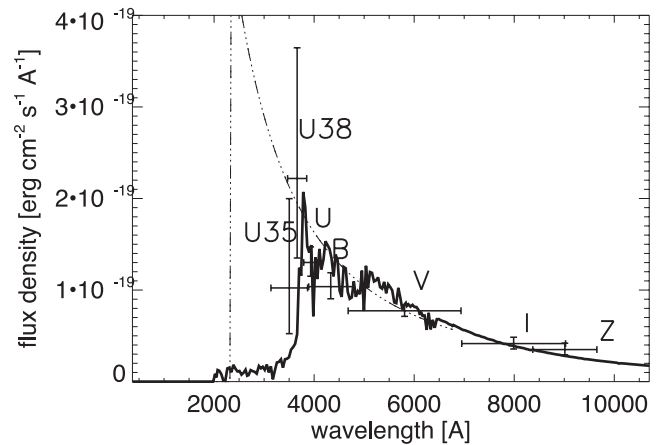


Figure 3. Best fit to the broad-band fluxes for galaxy B&C with filters WFI U35, U38, *U*_{VIMOS} and *HST* ACS *B*, *V*, *I* and *Z*. The thick solid line shows a Starburst99 model spectrum (Leitherer et al. 1999) with total stellar mass $1.4 \times 10^7 M_{\odot}$ and an age of $2 \times 10^6 \text{ yr}$, redshifted to $z = 3.0449$ and attenuated by the average Ly α forest opacity bluewards of 1215.67 Å in the rest frame. The dash-dotted line is meant to illustrate a hypothetical flat spectrum ($\beta = -2$) source at $z = 2.310$ (ignoring intergalactic absorption above the Lyman limit).

Starburst99 models (Leitherer et al. 1999). Absorption by the Ly α forest was taken into account by using the ‘MC-Kim’ transmission of Bershadsky et al. (1999).

An instantaneous starburst with the Starburst99 default standard initial mass function (IMF), an age of $2.0 \times 10^6 \text{ yr}$ and a total stellar mass of $1.4 \times 10^7 M_{\odot}$ fits the observed spectral energy distribution (SED) with a χ^2 corresponding to an 11 per cent probability (with the total flux being the only free parameter). More extreme stellar populations can in principle improve the fit further. Choosing an extreme IMF that is flat or consists of only massive stars ($M > 5 M_{\odot}$) and an age of the burst of only $1.4 \times 10^6 \text{ yr}$ would increase the flux near the Lyman limit further and produce a χ^2 probability of about 30 per cent, but may not be warranted on physical grounds.

Fig. 3 shows a comparison between the observed fluxes and the best-fitting model spectrum. For illustrative purposes, the dash-dotted line also shows a flat (in f_{ν}) spectrum at lower redshift ($z = 2.310$) (ignoring Ly α forest absorption), as if the object were at the photometric redshift derived by Cardamone et al. (2010). From this comparison it is not surprising that a large uncertainty in the *U*-band flux, with filters straddling the Lyman limit, can lead to a degeneracy in redshift. We conclude that the observations of the B&C object are consistent with it being a galaxy at the redshift of the QSO if we assume the presence of a very young population of stars.

We do not know the lifetime of the QSO, but can estimate crudely the possibility of finding two ‘young objects’ (the QSO and object B&C) as close together as observed. The probability distribution of a chance coincidence of a second object with a magnitude $V < 27$ and $B - V < 0.35$ (as observed for B&C) to occur near a similarly ‘blue’ pre-selected object, estimated from random draws from the Giavalisco et al. (2004) galaxy catalogue, makes the present arrangement approximately a 3.4σ excursion. More severe upper limits on the chance probability of finding a (short-lived) AGN and a short-lived population of young stars can be derived from the respective duty cycles. Assuming a duty cycle of a few per cent for QSOs (Nandra et al. 2002; Yu & Tremaine 2002) and ~ 6 per cent for starbursts in dwarf galaxies (Lee et al. 2009) gives a sub-percent

probability for finding both in the active stage. Thus, if the galaxy indeed has a young stellar population, its formation must be closely coeval with the QSO activity.

3 THE ORIGIN OF THE Ly α EMISSION

Producing the observed Ly α fluxes in the features 1 and 2 outside the main QSO emission line through recombination following photoionization requires an ionization rate

$$\dot{N}_{\text{ion}} = \frac{3}{2} \left(\frac{F_{\text{Ly}\alpha}}{h\nu_{\text{Ly}\alpha}} \right) 4\pi D_L^2 = 1.2 \times 10^{52} \left(\frac{F_{\text{Ly}\alpha}}{1.5 \times 10^{-18}} \right) \text{ s}^{-1}, \quad (1)$$

where a case B conversion from ionizing photons into Ly α photons has been assumed, and the combined Ly α flux $F_{\text{Ly}\alpha}$ of objects 1 and 2 is $(1.5 \pm 0.3) \times 10^{-18} \text{ erg cm}^{-2} \text{ s}^{-1}$. D_L is the luminosity distance at $z = 3.045$. The stellar population of object B&C, at a magnitude $m_{\text{AB}} = 26.6$ in the observed V band, produces H I ionizing photons at a rate of approximately $1.55 \times 10^{53} \text{ s}^{-1}$ (using the assumptions made in Paper I). Thus, the supply of ionizing photons, if completely trapped in the gaseous haloes of B&C and converted into Ly α as assumed above, would exceed the number of ionizations required to explain the observed Ly α emission by a comfortable factor of 13 (ignoring slit losses for Ly α).

Alternatively, the Ly α emission from objects 1 and 2 could, in principle, also be powered by the QSO. The spatially extended, diffuse Ly α emission centred on the QSO extends more than half the distance between the QSO and objects 1 and 2 at a similar surface brightness level. This suggests that the ionizing flux from the QSO is at least in some directions of the same order of magnitude as required to power the Ly α emission of objects 1 and 2.

4 CONCLUSIONS

The asymmetric extent of the Ly α halo is common for ‘fuzz’ around QSOs (e.g. Christensen et al. 2006), presumably reflecting the tilt of the ionization cone away from the line of sight to the observer. We have argued that the extension of the halo in the direction of the B&C object and the alignment of the spatial substructure in the Ly α emission with the broad-band imaging positions of the galaxy suggest a physical proximity and possible causal connection between the QSO and the object. Coeval activity is further suggested by the coincidence between apparently recent star formation and the active state of the QSO. The similarity of the lobes of B&C in brightness and colours suggests that they may constitute a single coherent galaxy, with the velocity difference of 290 km s^{-1} perhaps being due to rotation. The appearance of two spatially distinct Ly α emission regions for this object as opposed to a common halo may simply reflect the two discrete stellar regions. Alternatively, the separate Ly α peaks may be caused when the Ly α emission gets suppressed in the centre of the B&C structure either by the QSO physically expelling the gas or by largely ionizing it. In either case, any further ionizing radiation may just pass through the cleared patch and not be available for conversion to Ly α . As for the hole in the stellar population, it is not clear how this could be produced after the stars are already in place, but it does appear more likely that the QSO may determine in the first place where the stars are to be formed (and where not). If feedback from the QSO is influencing the properties of this object, then the fact that the structure is largely symmetric must either be a fortunate coincidence (e.g. a chance alignment with whatever symmetry the QSO feedback mechanism possesses, such as a jet that just happens to hit the galaxy at the right spot) or the structure with its stars and gas distribution must

be formed as a direct result of the QSO feedback. In the latter case, the star formation geometry naturally reflects the directional symmetry of the feedback. Such a possibility has been suggested in the literature (see the introduction), both to explain the observational alignments of star-forming regions and outflows from radio galaxies, and as a theoretically predicted consequence of AGN feedback. It appears that the current case may be a high-redshift candidate case for AGN-induced star formation in an external galaxy. This interpretation, if confirmed, would be consistent with the idea discussed in Papers I and II, that asymmetric, extended Ly α emitters trace a crucial phase in the galaxy formation process, where interactions among the building blocks of future normal galaxies influence the gas dynamics, star formation process and production of ionizing radiation in these objects.

ACKNOWLEDGEMENTS

We acknowledge helpful discussions with Carolin Cardamone, Andrea Grazian and Francois Schweizer. We thank the staff of the Las Campanas Observatory for their help with the observations. MR is grateful to the IoA in Cambridge and to the Raymond and Beverley Sackler Distinguished Visitor programme for hospitality and support in summer 2011 and 2012, when some of this work was done, and to the National Science Foundation for grant AST-1108815. GB has been supported by the Kavli Foundation. JRG acknowledges a Millikan Fellowship at Caltech. We acknowledge the use of the extinction calculator by Doug Welch.¹

REFERENCES

- Begelman M. C., Cioffi D. F., 1989, *ApJ*, 345, 21
- Bershady M. A., Charlton J. C., Geoffroy J. M., 1999, *ApJ*, 518, 103
- Brusa M. et al., 2009, *ApJ*, 693, 8
- Cardamone C. N. et al., 2010, *ApJS*, 189, 270
- Chambers K. C., Miley G. K., van Breugel W., 1987, *Nat*, 329, 604
- Christensen L., Jahnke K., Wisotzki L., Sanchez S. F., 2006, *A&A*, 459, 717
- Croft S. et al., 2006, *ApJ*, 647, 1040
- De Young D. S., 1981, *Nat*, 293, 43
- De Young D. S., 1989, *ApJ*, 342, L59
- Dey A., van Breugel W., Vacca W. D., Antonucci R., 1997, *ApJ*, 490, 698
- Efremov Y. N., 2013, *MNRAS*, 429, L75
- Fabian A. C., 1999, *MNRAS*, 308, 39
- Farrah D. et al., 2012, *ApJ*, 745, 178
- Fragile P. C., Murray S. D., Anninos P., van Breugel W., 2004, *ApJ*, 604, 74
- Gaibler V., Khochfar S., Krause M., Silk J., 2012, *MNRAS*, 425, 438
- Giavalisco M. et al. (GOODS Team), 2004, *ApJ*, 600, L93
- Grazian A. et al., 2006, *A&A*, 449, 951
- Haiman Z., Rees M. J., 2001, *ApJ*, 556, 87
- Hildebrandt H. et al., 2006, *A&A*, 452, 1121
- Lee J. C., Kennicutt R. C. Jr., Funes S. J., Jose G., Sakai S., Akiyama S., 2009, *ApJ*, 692, 1305
- Leitherer C. et al., 1999, *ApJS*, 123, 3
- Luo B. et al., 2010, *ApJS*, 187, 560
- Maiolino R. et al., 2012, *MNRAS*, 425, 66
- McCarthy P. J., van Breugel W., Spinrad H., Djorgovski S., 1987, *ApJ*, 321, 29
- Mellema G., Kurk, Röttgering H. J. A., 2002, *A&A*, 395, L13
- Nandra K., Mushotzky R. F., Arnaud K., Steidel C. C., Adelberger K. L., Gardner J. P., Teplitz H. I., Windhorst R. A., 2002, *ApJ*, 576, 625
- Padovani P., Allen M. G., Rosati P., Walton N. A., 2004, *A&A*, 424, 545
- Rauch M., Becker G. D., Haehnelt M. G., Gauthier J.-R., Ravindranath S., Sargent W. L. W., 2011, *MNRAS*, 418, 1115 (Paper I)

¹ <http://dogwood.physics.mcmaster.ca/Acurve.html>

Rauch M., Becker G. D., Haehnelt M. G., Gauthier J.-R., Sargent W. L. W.,
2013, MNRAS, 429, 429 (Paper II)
Rees M. J., 1989, MNRAS, 231, 1
Schawinski K., Virani S., Simmons B., Urry C. M., Treister E., Kaviraj S.,
Kushkuley B., 2009, ApJ, 692, 19
Silk J., 2005, MNRAS, 364, 1337
Silk J., Rees M. J., 1998, A&A, 331, 1
Szokoly G. P. et al., 2004, ApJS, 155, 271
Treister E. et al., 2006, ApJ, 640, 603
van Breugel W., Filippenko A. V., Heckman T., Miley G., 1985, ApJ, 293,
83

Vanzella E. et al., 2010, ApJ, 725, 1011
Wolf C., Dye S., Kleinheinrich M., Meisenheimer K., Rix H.-W., Wisotzki
L., 2001, A&A, 377, 442
Xue Y. Q. et al., 2011, ApJS, 195, 10
Yu Q., Tremaine S., 2002, MNRAS, 335, 965
Zheng W. et al., 2004, ApJS, 155, 73

This paper has been typeset from a $\text{T}_{\text{E}}\text{X}/\text{L}^{\text{A}}\text{T}_{\text{E}}\text{X}$ file prepared by the author.